frontiers | Frontiers in Earth Science

ORIGINAL RESEARCH
published: 22 June 2022
doi: 10.3389/feart.2022.914383

Classification and Evaluation of Volcanic Rock Reservoirs Based on the Constraints of Energy Storage Coefficient

Wen-Tie Sun[1,2,3], *Yi-Shan Lou*[1,2], *Arnaud Regis Kamgue Lenwoue*[1,2], *Zhong-Hui Li*[1,2]*, *Liang Zhu*[1,2] *and Hui-Mei Wu*[1,2]

[1]*Department of Petroleum Engineering, Leak Resistance and Sealing Technology Research Department National Engineering Laboratory of Petroleum Drilling Technology, Yangtze University, Wuhan, China,* [2]*Key Laboratory of Drilling and Production Engineering for Oil and Gas, Wuhan, China,* [3]*Exploration and Development Research Institute of Jilin Oil Field Company, PetroChina, Songyuan, China*

OPEN ACCESS

Edited by:
Hu Li,
Southwest Petroleum University, China

Reviewed by:
Cunhui Fan,
Southwest Petroleum University, China
Kun Zhang,
Southwest Petroleum University, China

***Correspondence:**
Zhong-Hui Li
lizc577@126.com

Specialty section:
This article was submitted to Structural Geology and Tectonics, a section of the journal Frontiers in Earth Science

Received: *06 April 2022*
Accepted: *02 May 2022*
Published: *22 June 2022*

Citation:
Sun W-T, Lou Y-S, Kamgue Lenwoue AR, Li Z-H, Zhu L and Wu H-M (2022) Classification and Evaluation of Volcanic Rock Reservoirs Based on the Constraints of Energy Storage Coefficient. Front. Earth Sci. 10:914383. doi: 10.3389/feart.2022.914383

The current classification and evaluation methods of volcanic rock reservoirs have low accuracy and cannot effectively provide guidance for the selection of volcanic rock gas reservoirs, which have efficient properties for gas production. In this research, we have analyzed the lithology, lithofacies, reservoir space type, pore combination mode, and reservoir microscopic characteristics of volcanic reservoirs using the energy storage coefficient as a constraint. Then, the method of reservoir classification was proposed. The results showed the following: 1) The energy storage coefficient can better characterize the single-layer productivity of gas wells. The volcanic rock reservoirs in the Wangfu gas field can be subdivided into three categories by considering the energy storage coefficient. 2) Type I reservoirs mainly develop structural fractures–matrix dissolution pores, structural fractures–intercrystalline micropores, and matrix dissolution pores. Type II reservoirs mainly develop matrix dissolution pores and residual intergranular pores, and Type III reservoirs are dominated by structural fractures. From Type I to Type III reservoirs, the skewness of the mercury intrusion curve and the sorting coefficient deteriorated, and the physical properties of the reservoir and the maximum mercury saturation and other parameters also decreased, whereas the displacement pressure and the median saturation pressure increased. 3) The characteristics of conventional and special logging curves of typical reservoirs were comprehensively analyzed, and the combination of sensitivity parameters reflecting gas-bearing properties and logging curves was optimized. Furthermore, a reservoir classification chart was established, and the results enabled to confirm the choice of the reservoir and demonstrated that the standard classification has high accuracy. 4) The diagenesis processes such as weathering, leaching, and dissolution improved the physical properties of the reservoir. The research results can effectively provide guidance for the evaluation of the “sweet spot” of volcanic rock reservoirs.

Keywords: reservoir classification, energy storage factor, volcanic rocks, wangfu gas field, diagenesis

1 INTRODUCTION

With the increasing global demand for oil and natural gas resources, unconventional oil and gas resources, such as volcanic gas reservoirs, have become a new field for global oil and gas exploration and development (Stagpoole et al., 2001; Polyansky et al., 2003; Feng et al., 2006; Wu et al., 2006; Shi B. et al., 2020). China has become the main subject for the global volcanic rock oil and gas reservoir exploration practice and has made major breakthroughs in the exploration of volcanic rocks in the Songliao basin, Sichuan basin, and Junggar basin (Feng et al., 2008; Feng et al., 2014; Gao, 2019; Li, 2022; Mao et al., 2015; Chang et al., 2019; Wen et al., 2019). In the Songliao basin, a number of volcanic rock oil and gas reservoirs have been discovered, which showed great potential for oil and gas. The results of gas testing and production have confirmed that volcanic gas reservoirs have large differences in gas well productivity.

Reservoir characteristics are mainly studied in terms of lithology, lithofacies, reservoir space types, pore combinations, pore structures, and reservoir classification scheme (Lan et al., 2021; Pola et al., 2012; Wang et al., 2015; Li et al., 2019; Gao, 2019; Li, 2022; Sruoga and Rubinstein, 2007; Shi et al., 2020b; Zheng et al., 2018b). The lithology identifications of volcanic rock mainly include three methods: gravity-magnetic-electric method identification, geological-log data identification, and seismic identification method (Ran et al., 2005; Chen et al., 2010; Gong et al., 2012). Wang et al. (2006) stipulated that volcanic rocks can be divided into basic, neutral, and acidic volcanic rocks according to the differences in the mineral composition. According to the diagenetic method, the rocks are divided into lava, clastic lava, and pyroclastic rocks; Wang et al. (2003a), Luo et al. (2008), Mou et al. (2010) divided the volcanic lithofacies into 5 types and 15 subfacies according to the volcanic eruption modes, rock types, and volcanic rock output forms. Ren and Jin (1999), Wang et al. (2014), and Luo et al. (2008) divided the reservoir space into primary pores and fractures, and secondary pores and fractures according to the morphological characteristics. Yu et al. (2004) pointed out that in the volcanic rock reservoir space, there are various combinations of pores and fractures. The main technical means for studying the microstructures of the volcanic reservoir space include the capillary pressure curve method, cast thin section, scanning electron microscope, CT scanning, resistivity logging, and nuclear magnetic resonance logging methods (Sruoga and Rubinstein, 2007; Shi et al., 2020b; Zheng et al., 2018b; Hou et al., 2020; Tian et al., 2013; Ma et al., 2017; Yin and Wu., 2020). Sruoga et al. (2004) studied the controlling effect of diagenesis on porosity and permeability in volcanic rock reservoirs by taking the Neuque'n basin in southern Argentina as an example; Pang et al. (2007) analyzed the microscopic pore structures of acid volcanic rock reservoirs and used mercury intrusion data to divide the pore structures of the Yingcheng Formation volcanic rocks in the northern Songliao basin into coarse and fine types.

At present, the classification and evaluation standards of volcanic rock reservoirs are not uniformized. Liu et al. (2003) applied the principle of fuzzy mathematics to select three parameters of energy storage abundance, permeability, and median pore-throat radius that reflect the macroscopic and microscopic characteristics of the reservoir and established the reservoir selection on the basis of core analysis and test data. Evaluation criteria of volcanic rock reservoirs and reasonable structural membership functions included calculating weights and selecting appropriate fuzzy synthesis. Shan et al. (2011) selected seven key parameters for reservoir evaluation based on the factors affecting the quality of volcanic rock reservoirs. They assigned parameters based on expert experience and conducted a single-well reservoir quantitative evaluation. Jin et al. (2007), Chen et al. (2016), and Huang et al. (2019) established the classification and evaluation standards of volcanic rock reservoirs by considering the lithology, storage space combination, physical, electrical, and gas-bearing properties. At present, the accuracy of classification of volcanic rock reservoirs is not high. In fact, compared with clastic rock reservoirs, volcanic rock reservoirs have strong reservoir heterogeneity and are mainly characterized by multi-layer production. In the process of fracturing and production, low-efficiency layers lead to increasing investment costs and low production of gas wells. This paper carries out quantitative and qualitative descriptions of volcanic rock reservoirs and establishes a set of evaluation criteria for effective reservoir classification, and the research results can effectively provide guidance for the evaluation of the "sweet spot" of volcanic rock reservoirs.

2 REGIONAL OVERVIEW, EXPERIMENTAL EQUIPMENT, AND METHODS

2.1 Geological Background

The Wangfu gas field is located in the northwest of the southeast uplift area in the southern Songliao basin. The exploration area is 2,100 km^2. The overall structural form is characterized by steep in the west and gentle in the east. Seismic data and drilling parameters revealed that the Paleozoic Carboniferous–Permian strata are developed from bottom to top in the study area, including the upper Jurassic Huoshiling Formation, lower Cretaceous Shahezi Formation, Yingcheng Formation, Denglouku Formation, and Quantou Formation. The first and second sets of strata are presented in **Figure 1**.

The research horizons are the Shahezi and Huoshiling Formations. A total of 29 wells in the study area revealed that the thickness of the formation is 160–1,223 m. The study area has experienced four stages of volcanic eruption (**Figure 2**). The eruption stages I to III were formed in the period of the Huoshiling Formation and were formed by central-fissure volcanic eruptions. It is mainly composed of rock, trachoic breccia and submerged volcanic breccia, and andesite, and basalt, which are locally developed; the eruption stage IV was formed in the Shahezi Formation, and it is only developed in the structural high of the CS6 well area. The lithology is submerged by volcanic breccia, and the scale of the volcanic body is small.

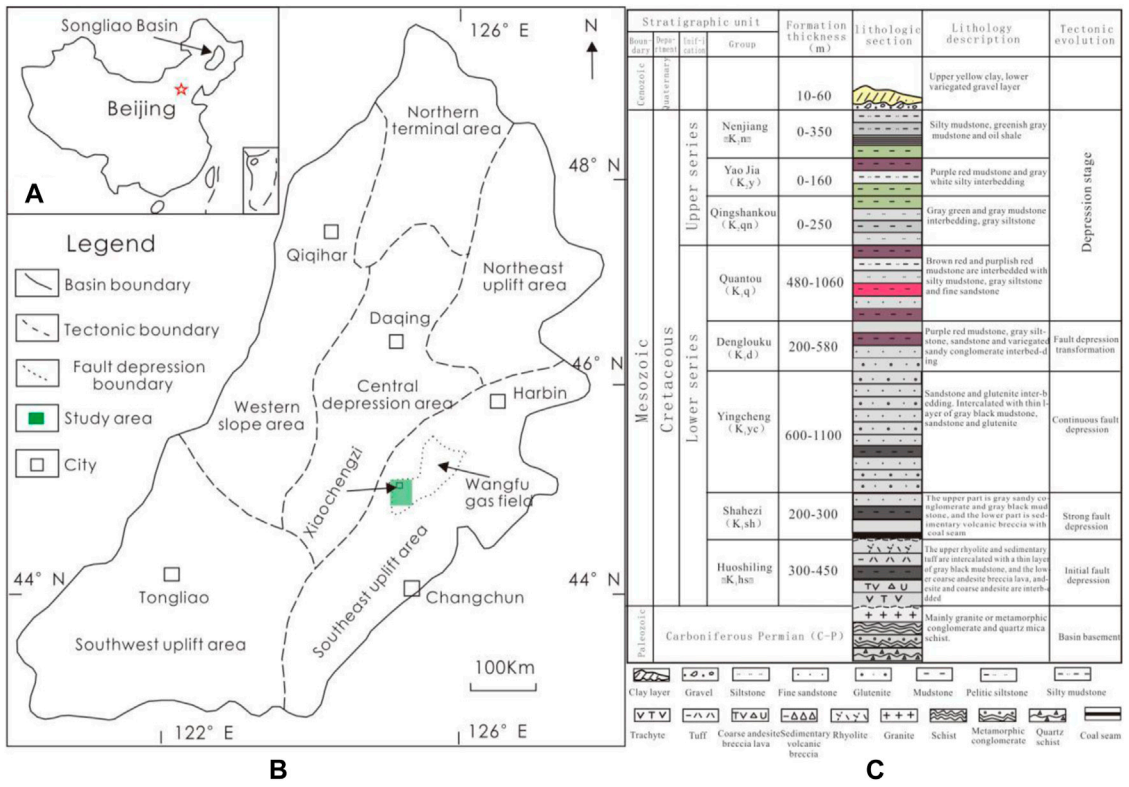

FIGURE 1 | (A) Geographical location map of the Songliao basin, **(B)** regional structural location map of the Wangfu gas field, and **(C)** comprehensive stratigraphic bar map of the Wangfu gas field.

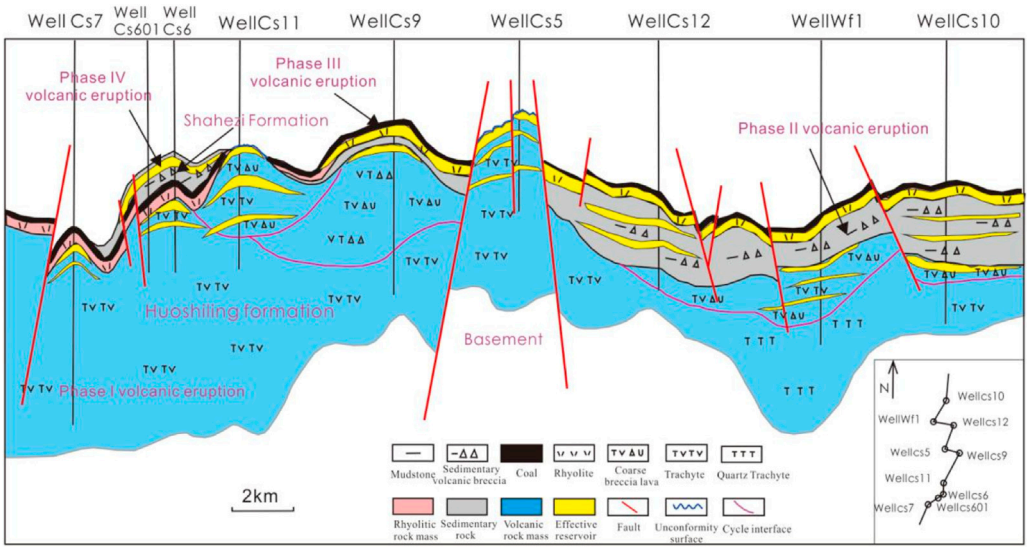

FIGURE 2 | Contrastive profile of volcanic rocks in the Wangfu gas field through wellCs7 to wellCs10.

2.2 Experiments and Methods

During the exploration of this area, seismic, logging, drilling, and test data were obtained. The lithology of volcanic rocks in 29 wells was identified using 271 m cores, 124 cast thin sections, and 4,030 m full borehole imaging logging data (FMI–Formation MicroScanner Image); the lithofacies of volcanic rocks were identified by a combination of geological and logging data. The types of reservoir spaces and pores were observed through resin-impregnated core

samples and cast thin sections. The pore structure characteristics of the volcanic rock reservoirs were analyzed using the data of 26 ordinary mercury injection experiments. This study selected a core sample that has good representativeness. The high-quality volcanic rock reservoir is mainly formed in the weathering crust at the top of volcanic eruption period. The diagenesis of weathering forest filtration and dissolution has a great influence on the reservoir physical property, while the burial depth has a little influence on the reservoir. Meanwhile, in order to further eliminate the influence of burial depth, core samples are mainly selected from the weathered crust, as detailed in **Section 5.2**.

Porosity and permeability tests were performed at the Physics Laboratory of Jilin University, Changchun City, Jilin Province, using the AP608 instrument through helium (helium) injection. The test temperature was 220°C, and the test was carried out in accordance with the standard method of petroleum industry of the People's Republic of China (SY/T 5336–2006, "Core Analysis Method").

The capillary pressure was measured by mercury porosimetry using an automated IV 9505 porosity analyzer in the Fluid Mechanics Laboratory of the Daqing Oilfield Research Institute. The test temperature was 19.10°C, and the humidity was 39% RH. The test adopts the petroleum industry standard method of the People's Republic of China (SY/T 5346-2005: "Measurement of the capillary pressure curve of rocks").

The reservoirs' characteristics of intrusive rocks were analyzed by the integration analysis of petrology, logging, and 3D seismic. The void spaces were assessed through a combination of megascopic observations, thin section of resin-impregnated studies of samples from 8.5 m core of intrusive rocks of the Huoshiling Formation of the Wangfu gas field.

3 CHARACTERISTICS OF VOLCANIC RESERVOIRS

3.1 Lithology and Lithofacies

Lithology is the basic parameter for evaluation of volcanic reservoirs (Sun et al., 2019). The Wangfu gas field volcanic rocks have complex lithology and rock types. On the basis of identifications of cores and cast thin sections, the three-level classification principle of "genesis + composition + structure" is adopted. The volcanic rocks have been divided into four categories: volcanic lava, pyroclastic rock, volcanic lava–volcanic clastic rock, and pyroclastic rock–sedimentary rock.

The volcanic lava reservoirs include six lithologies: trachyandesite, andesite, trachyte, basalt, dacite, and rhyolite. Among them, trachyandesite and andesite are the most developed accounting for 43.74%, while the other lithologies are relatively few, accounting for less than 10%. Pyroclastic reservoirs are mainly present in coarse andesitic (tuff) volcanic breccia, andesitic volcanic breccia (tuff), rhyolitic (tuff) volcanic breccia, and trachytic (tuff) volcanic breccia. Among them, coarse andesitic (tuff) volcanic breccia and andesitic volcanic breccia (tuff) are moderately present, accounting for 12.78 and 8.48%, respectively. The volcanic clastic rock reservoirs are mainly encountered in coarse andesitic (tuff) breccia lava and andesitic (tuff) breccia lava, accounting for 7.88 and 4.37%, respectively. The clastic rock–sedimentary rock reservoirs are mainly composed of sedimentary pyroclastic rock, accounting for 10.56% (**Figure 3**).

The study area mainly includes four types of volcanic lithofacies: explosive facies, overflow facies, volcanic channel facies, and volcanic sedimentary facies. The results in **Figure 4** show that the upper, middle, and lower subfacies of the overflow facies are encountered in the whole area, accounting for 67.4%; the proportion of pyroclastic flow in explosive facies is 19.6%, and there are few empty falling subfacies. Volcanic neck subfacies and re-transported pyroclastic sedimentary rocks are relatively few.

3.2 Types of Storage Space

According to the classification scheme of storage space types by Wang et al. (2003b), He et al. (2016), and Tang et al. (2020), the storage space of volcanic rocks in the Wangfu gas field can be divided into primary and secondary categories: Combined with the structure and morphology of the reservoir space, it can be further subdivided into four subtypes: primary pores, primary fractures, secondary pores, and secondary fractures. There are 10 types of specifically identified reservoir spaces, including primary pores, intergranular pores, intercrystalline micropores, explosion fractures, phenocryst pores, matrix corrosion pores, dissolution fractures, and structural fractures (**Table 1**; **Figure 5**).

4 CLASSIFICATION AND EVALUATION OF VOLCANIC RESERVOIR

4.1 Analysis on Influencing Factors of Volcanic Reservoir

Reservoir classification is an important part of high-quality reservoir screening and is also a key step in establishing high-quality reservoir identification criteria (Zhao et al., 2007; Wang et al., 2021). There are many factors that affect the productivity of gas wells. The geological parameters used to classify the volcano reservoir sweet spot are reasonable and easy to operate. Therefore, the test data of 10 wells in the Wangfu gas field (**Table 2**) are obtained for effective thickness (H), effective thickness * porosity (h.Φ), formation coefficient (h.k), and energy storage coefficient ($h.\Phi.S_{g_i}$). The relationship between other parameters and unblocked flowrate is studied, and the sensitive parameters to reservoir characteristics are implemented.

4.1.1 Single Layer Production Splitting (Q_i)

The volcanic reservoir is characterized by strong reservoir heterogeneity and "thin and multi-layer" lithologic combination. In the production process, in order to achieve a certain output of a single gas well, it is necessary to increase the productivity by multi-layer joint investment. In order to distinguish the contribution of single-layer natural gas production, it is necessary to split the production volume (Wang et al., 2016; Kadavi et al., 2018; Yang et al., 2018; Faizan et al., 2019). In this study, the parameter method is used to split the output. The formula is as follows:

$$Q_i = Q_0.\frac{h_i.\Phi_i.S_{g_i}}{\sum_i^n h.\Phi.S_g}, \quad (1)$$

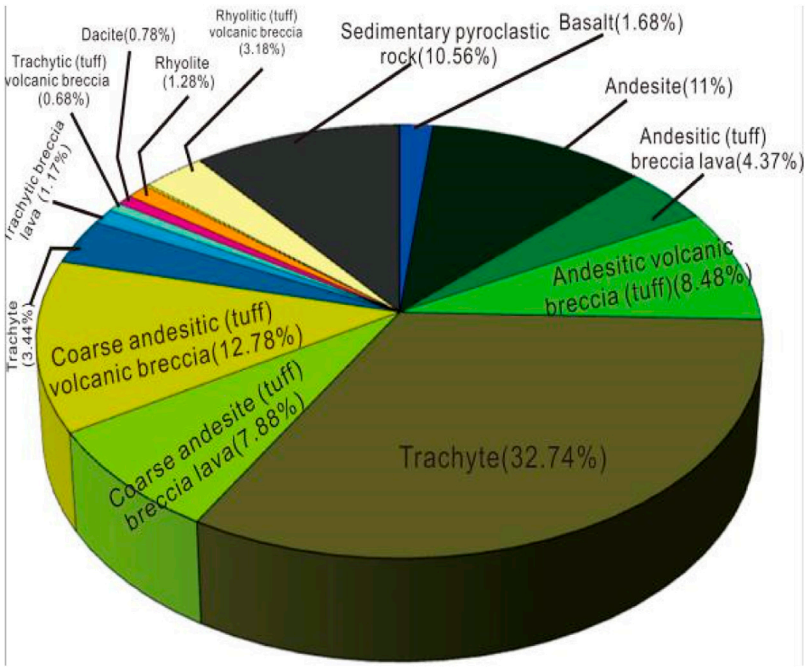

FIGURE 3 | Pie chart of volcanic rock lithology distribution in the Wangfu gas field.

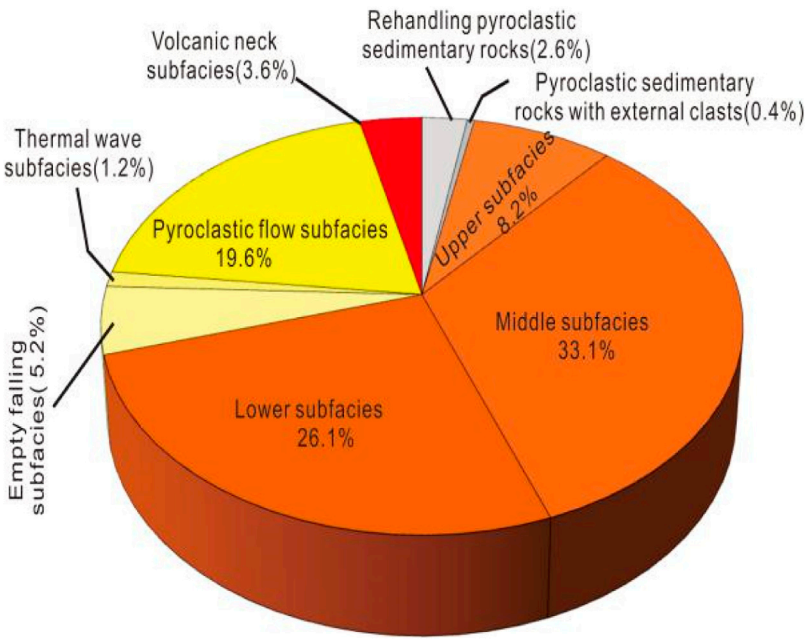

FIGURE 4 | Pie chart of volcanic lithofacies distribution in the Wangfu gas field.

where Q_0—test production (10^4 m^3), Q_i—level i test production (10^4 m^3), h—average effective thickness (m), Φ—average effective porosity (%), S_g—average original gas saturation (%), h_i—average effective thickness of layer i (m), Φ_i—average effective porosity of layer i (%), and S_{g_i}—average original gas saturation of layer i (%).

4.1.2 Effective Thickness (H)

Effective thickness refers to the thickness of the gas reservoir with gas production capacity under the production differential pressure allowed by the existing process technology. Generally, the effective thickness is directly proportional to the gas well

TABLE 1 | Reservoir space types and characteristics of the volcanic rocks in the Huoshiling Formation of the Wangfu gas field in the Songliao basin.

Type of Storage Space			Genesis Mechanism	Characteristics	Distribution	Representative Legend
Primary	Pores	Primary pore	Formation of volatile gas escape	The shapes of stomata are round, oval, and irregular, with different sizes, and some of them are unconnected independent pores	It is mostly found in rhyolite and trachyte in the upper and lower subfacies of eruptive facies	**Figure 5A**
		Intergranular pore	Residual pores after compaction of pyroclastic particles	Irregular shape, usually distributed along the edge of debris, with good connectivity	Volcano clastic rocks are mainly pyroclastic subfacies and subsurface facies	**Figure 5B**
		Intercrystalline pore	Residual space after crystallization	It develops between lava matrix and microcrystalline minerals and can be seen under the microscope	Trachyte and andesite, the middle part of the eruption facies	**Figure 5C**
	Fracture	Explosion fracture	Phenocryst fissure caused by magmatic eruption	The crystal plane is irregular or cleavage like	Rhyolitic clastic rocks of explosive facies are common	**Figure 5D**
Secondary	Pores	Phenocryst pore	Formed by hydrothermal solution, groundwater dissolution, and weathering leaching	The pore shape is irregular, the minerals are completely dissolved, and the original crystal illusion is retained	All kinds of volcanic rocks, cycle times, top, fault zone, and uplift area	**Figure 5E**
		Matrix corrosion pore	Formed by hydrothermal solution, groundwater dissolution, and weathering leaching	The pore morphology is mostly small sieve pore with certain connectivity	All kinds of volcanic rocks, cycle times, top, fault zone, and uplift area	**Figure 5F**
	Fracture	Dissolution fracture	Formed by hydrothermal solution, water dissolution, and weathering leaching	It has no directionality, the fracture wall is irregular, and it often dissolves along the early cracks. Developed in various volcanic rocks	They are developed in volcano rocks, secondary cycles, fault zones, and uplift zones	**Figure 5G**
		Structural fracture	Formation of tectonic stress	Directional, multi-stage cross cutting, penetrating crystals, or pyroclastic particles, communicating with other primary pores	All kinds of volcanic rocks, near faults, and uplift areas	**Figure 5H**

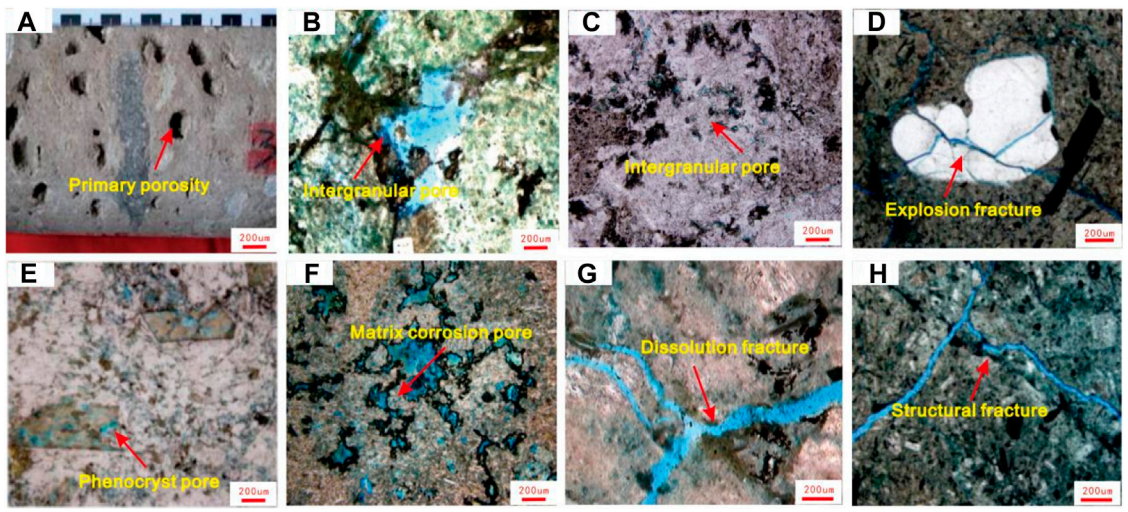

FIGURE 5 | Genetic types of volcanic rock reservoir space in the Wangfu gas field. **(A)** Primary pores, rhyolite, wellCs14, 2,997.75 m, core; **(B)** intergranular pores, rhyolite breccia, wellCs13, 2232mm, single polarized light×10; **(C)** intergranular pores, gray andesite, wellWf1, 3130m, single polarized light ×10; **(D)** explosion fracture, trachycere breccia lava, well Cs11, 3043m, single polarized light ×10; **(E)** porphyry pores, trachyandesite, wellWf1, 3230 m, single polarized light×10; **(F)** matrix corrosion pore, volcanic breccia, wellCs602, 2,614.8 m, single polarized light×10; **(G)** dissolution fracture, trachyandesite, wellCs11, 2720 m, single polarized light×10; and **(H)** structural fracture, trachoic breccia lava, wellCs11, 3043m, single polarized light×10.

production. Usually, the greater the effective thickness, the higher the gas well production (Zhou et al., 2007; Hasan et al., 2018). **Figure 6A** shows that there is a certain correlation between the effective thickness of volcanic reservoir and open flow, but the correlation coefficient R^2 is low, only 0.1548. This conclusion is quite different from the understanding of clastic reservoir. There

TABLE 2 | Statistics of the production capacity and sensitivity parameters of the Wangfu gas field reservoir.

Well Number	Test Production	Layer Number	Split Test Production Q_i ($\times 10^4$ m^3/d)	Porosity (%)	Permeability (mD)	Gas Saturation (%)	Effective Thickness (m)	Energy Storage Coefficient
WF1	8.9	219	0.373	4.6	0.15	45.0	2.6	0.05
		220	2.525	6.5	0.25	55.0	10.2	0.36
		240	5.050	5.5	0.15	60.0	22.1	0.73
		241	0.952	5.0	0.14	50.0	5.5	0.14
CS4	5.5	171	2.937	6.3	0.22	55.0	2.8	0.10
		172	0.839	5.7	0.17	40.5	1.2	0.03
		176	0.997	4.2	0.17	39.2	2	0.03
		179	0.728	3.8	0.21	45.2	1.4	0.02
CS5	12.8	78	0.452	8.7	0.80	38.7	1.3	0.04
		79	3.977	9.8	1.24	56.2	7	0.39
		80	8.371	8.2	0.63	53.2	18.6	0.81
CS6	16.2	148	10.329	13.8	3.83	65	11.6	1.04
		153	5.871	10.2	1.43	38	11	0.43
CS7	1.2	207	0.406	4	0.18	40	14.7	0.24
		208	0.587	4.5	0.15	46	16.4	0.34
		209	0.207	4.5	0.15	38	7	0.12
CS9	10.6	117	1.365	12.2	2.61	31.2	2.9	0.11
		116	4.722	16.1	5.96	50.6	4.7	0.38
		115	4.513	12.8	3.04	58.2	4.9	0.37
CS11	4.6	121	2.418	11.3	2.04	66.1	9.1	0.68
		107	2.182	8.4	0.69	58.6	12.5	0.61
CS601	3.5	161	1.509	5.0	0.14	62.7	14.7	0.46
		145	1.991	10.0	1.34	38.0	16	0.61
CS606	2.2	165	1.504	11.1	1.92	48.1	10.6	0.57
		163	0.696	8.3	0.66	38.0	8.3	0.26
CS608	1.9	175	1.900	18.0	8.17	50.0	6	0.54

are two main reasons: First, the formation of volcanic reservoir has a certain suddenness from the formation mechanism, and the distribution scale, lithology, physical properties, and pore structure characteristics of the volcanic reservoir have a strong non-mean, and it is difficult to determine the plane and longitudinal distribution law. At present, there is no corresponding research report, and this field will be the focus of further research. Second, compared with clastic reservoirs, the production of gas wells is not only related to the effective thickness of volcano reservoirs but is also highly influenced by the physical properties (porosity and permeability) of gas reservoirs. Therefore, the effective thickness of the volcanic rock reservoir has poor correlation with productivity.

4.1.3 Effective Thickness * Porosity (H.Φ)

Porosity is a parameter to measure the ability of the rock reservoir to contain fluids. The larger the porosity of reservoir, the larger the pore space in rock. Only the interconnected pores have practical significance from the practical point of view of gas reservoir research because they cannot only store natural gas but also allow gas to percolate therein. Therefore, the effective thickness of volcano reservoir * porosity (H.) is established. Φ) And open flow (**Figure 6B**).

From **Figure 6B**, it can be seen that when H Φ is greater than 0.43, the open flow is greater than $1.62 \times 10^4 m^3/d$, When H Φis close to or greater than 1.04, the open flow is greater than $3.74 \times 10^4 m^3/d$. h Φ. There is a certain positive correlation with the open flow, but the correlation coefficient R^2 is only 0.4915, which is still not ideal, and the correlation coefficient is still relatively low.

4.1.4 Formation Coefficient (H.K)

Permeability is the ability of rocks to allow fluids to pass through their pores. It plays an important role in studying and evaluating oil and gas reservoirs and production capacity (Farquharson et al., 2015). Therefore, the relationship between the formation coefficient (H.K) and open flow of volcanic reservoir in the Wangfu gas field is established. **Figure 6C** shows that the gas test production increases with the formation coefficient (H.K). When the local formation coefficient (H.K) is greater than 1.06, the open flow is greater than $1.62 \times 10^4 m^3/d$. However, the correlation coefficient R^2 between the formation coefficient and open flow is relatively low, only 0.3407, which is not ideal. The main reason is that the volcanic reservoir is dense and heterogeneous, and the production of gas wells is not only related to the effective thickness and physical properties, and it is also closely related to the gas bearing property of the gas reservoir. If there is a gas reservoir with large thickness and good physical properties, but with little gas or even water filled in it, the gas saturation will be low and the gas test will not obtain high production.

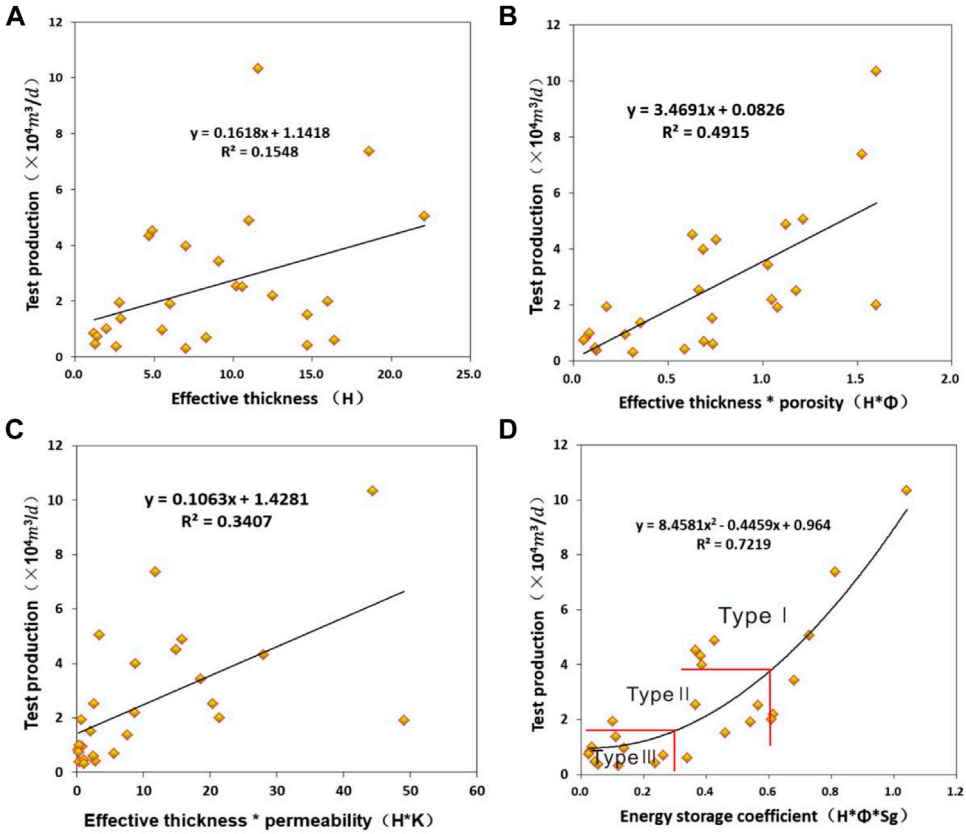

FIGURE 6 | Relationship between sensitive parameters and productivity of volcanic reservoir in the Wangfu gas field. Note: **(A)** Relationship between the effective thickness and production capacity, **(B)** relationship between effective thickness * porosity and productivity, **(C)** relationship between the formation coefficient and productivity; and **(D)** relationship between the energy storage coefficient and productivity.

4.1.5 Energy Storage Coefficient ($h.\Phi.S_{g_i}$)

As we all know, the reserve calculation formula using the volumetric method is

$$G = 0.01A_g.h.\Phi.S_{g_i}\frac{P_i.T_{SC}}{P_{SC}.T.Z_i}, \quad (2)$$

where G—natural gas original geological reserves (10^8 m^3), A_g—gas bearing area (km^2), h—average effective thickness (m), Φ—average effective porosity (%), S_{g_i}—average original gas saturation (%), T—average formation temperature (K), T_{SC}—ground standard temperature T (K), P_i—average initial formation pressure (MPa), P_{SC}—surface standard pressure (MPa), and Z_i—original gas deviation coefficient, a dimensionless quantity.

It can be seen from the formula that the energy storage coefficient ($h.\Phi.S_{g_i}$) is a factor of G, which better reflects the gas enrichment degree of a single horizon. **Figure 6D** shows that the energy storage coefficient has a good correlation with the gas well productivity. With the increase of energy storage coefficient, the gas well productivity increases in a polynomial relationship, and the correlation coefficient R^2 reaches 0.7219. Therefore, the energy storage coefficient can well reflect the productivity characteristics of the monolayer. When the energy storage coefficient is between 0.0 and 0.3, the open flow of the gas well is less than $1.62 \times 10^4 m^3/d$ (Class III). When the energy storage coefficient is between 0.3 and 0.6, the open flow of the gas well is in the range of $1.62 - 3.74 \times 10^4 m^3/d$(class II). When the energy storage coefficient is greater than 0.6, the open flow is more than $3.74 \times 10^4 m^3/d$ (class I) (**Figure 6D** and **Table 2**).

The gas test and production data of 10 wells in the study area were utilized to investigate the energy storage coefficient. Based on previous research and considering the energy storage coefficient as the constraint condition, the volcanic reservoir is divided into three categories according to the boundary of energy storage coefficient greater than 0.6, 0.6–0.3, and less than 0.3. The rock samples from different reservoirs were selected to complete the indoor experiments such as casting thin section and conventional mercury injection.

Based on the characteristics of conventional and special logging curves, the reservoir space combination characteristics were analyzed, the micro-pore structure and logging response characteristics of different types of reservoirs were evaluated, and the sensitive parameters such as the reflecting gas bearing property was optimized. Furthermore, the reservoir classification standards were established, and a guidance for the classification and evaluation of volcanic reservoirs was provided.

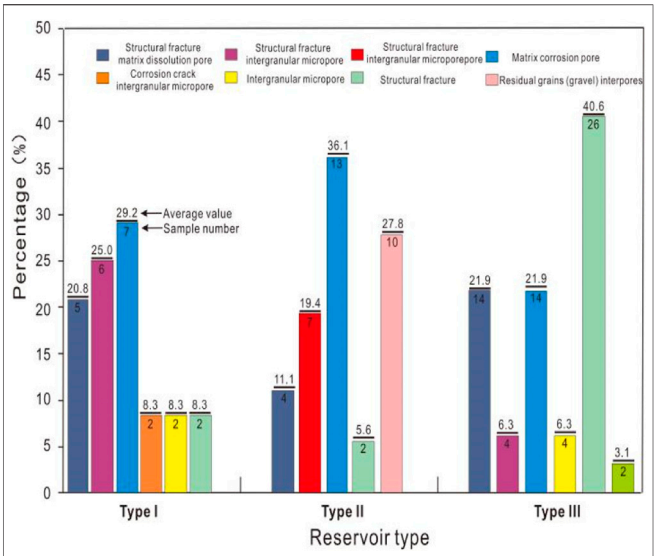

FIGURE 7 | Histogram of various reservoir spatial combinations of the volcanic reservoir in the Wangfu gas field.

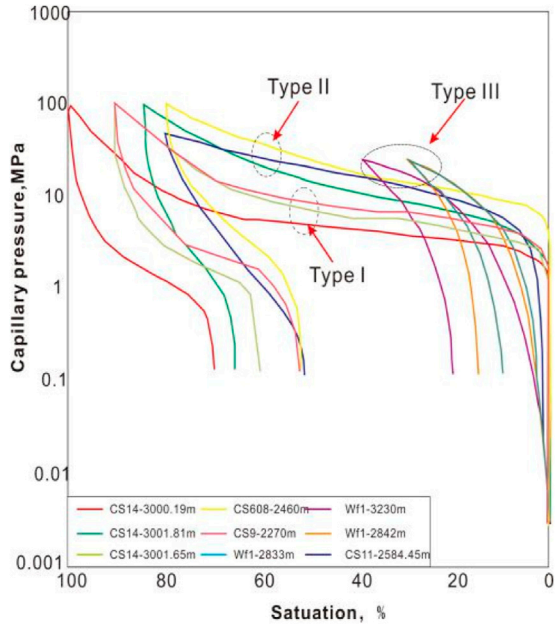

FIGURE 8 | Classification diagram of the mercury injection curve of the typical volcanic reservoir in the Wangfu gas field.

4.2 Reservoir Space Combination Characteristics

Generally, the reservoir space of volcanic rock reservoir does not exist alone but appears in some combination form (Zheng et al., 2018a; Wang et al., 2020). Therefore, using the data of 124 cast thin sections, the characteristics of the reservoir space combination are analyzed through image pore throat analysis and measurement technology, and the characteristics of reservoir space combination of three types of reservoirs are evaluated based on the dominant reservoir space combination (**Figure 7**).

Type I: This type is mainly composed of structural fracture matrix dissolution pores, structural fracture intergranular micropores, and matrix dissolution pores. Structural fracture matrix dissolution pores and structural fracture intergranular pores are common in andesite and rhyolite reservoirs of volcanic lava. Fractures play a connecting role between pores, and the reservoir space is greatly affected by the strength of dissolution and the magnitude of structural stress. Intergranular dissolution pores are often found in the andesite of volcanic lava reservoirs. The pores have good connectivity and strong seepage capacity and are generally good reservoir spaces.

Type II: Matrix dissolution pores and residual intergranular pores are mainly presented. The matrix dissolution pores and residual grains' interpores are mainly developed in the volcano clastic sedimentary rocks and volcano breccia reservoirs, which are affected by diagenesis and tectonics; the connectivity between pores is poor; the percolation ability is generally; and most of them are general reservoir spaces.

Type III: This type is mainly composed of structural fractures, followed by structural fractures' matrix dissolution pores and matrix dissolution pores. The type of structural fracture reservoir space is mostly the residual fractures after the structural fractures are filled with carbonate. The combination mode of reservoir space is single. This kind of pore structure is common in the pyroclastic rock reservoir and volcanic lava pyroclastic rock reservoir. The physical properties of the reservoir are poor, and most of them are poor reservoirs.

TABLE 3 | Typical mercury injection curves and characteristic parameters of volcano rocks with different pore throat types.

Classification of Pore Structure	Type I	Type II	Type III
PD (MPa)	<2.0	2.0–6.0	>6.0
Pc-50 (MPa)	<20.0	20.0–36.0	/
Maximum mercury saturation (%)	89.9–99.2	75.2–85.5	25–35
Porosity (%)	>8.0	4.0–8.0	<4.0
Permeability (mD)	>0.1	0.01–0.1	<0.01
Test production (× $10^4 m^3/d$)	<1.30	1.3–3.9	>3.9

4.3 Distribution Characteristics of Micro-Pore Structure

The genesis of volcanic reservoir throat is more complex than sedimentary rock, and the reservoir has different micro-pore structure characteristics. Based on the mercury injection data of 26 blocks, the micro-pore structure characteristics and seepage capacity of volcanic rock reservoir are analyzed. According to the pore structure and curve shape, the pore structure of the volcanic rock reservoir is divided into three categories (**Figure 8** and **Table 3**):

Type I: The curve shape is characterized by closing to the left and down and concave to the right, with coarse skewness and good sorting; The characteristic parameters are low displacement pressure (PD < 2 MPa), low mercury saturation median pressure (PD <

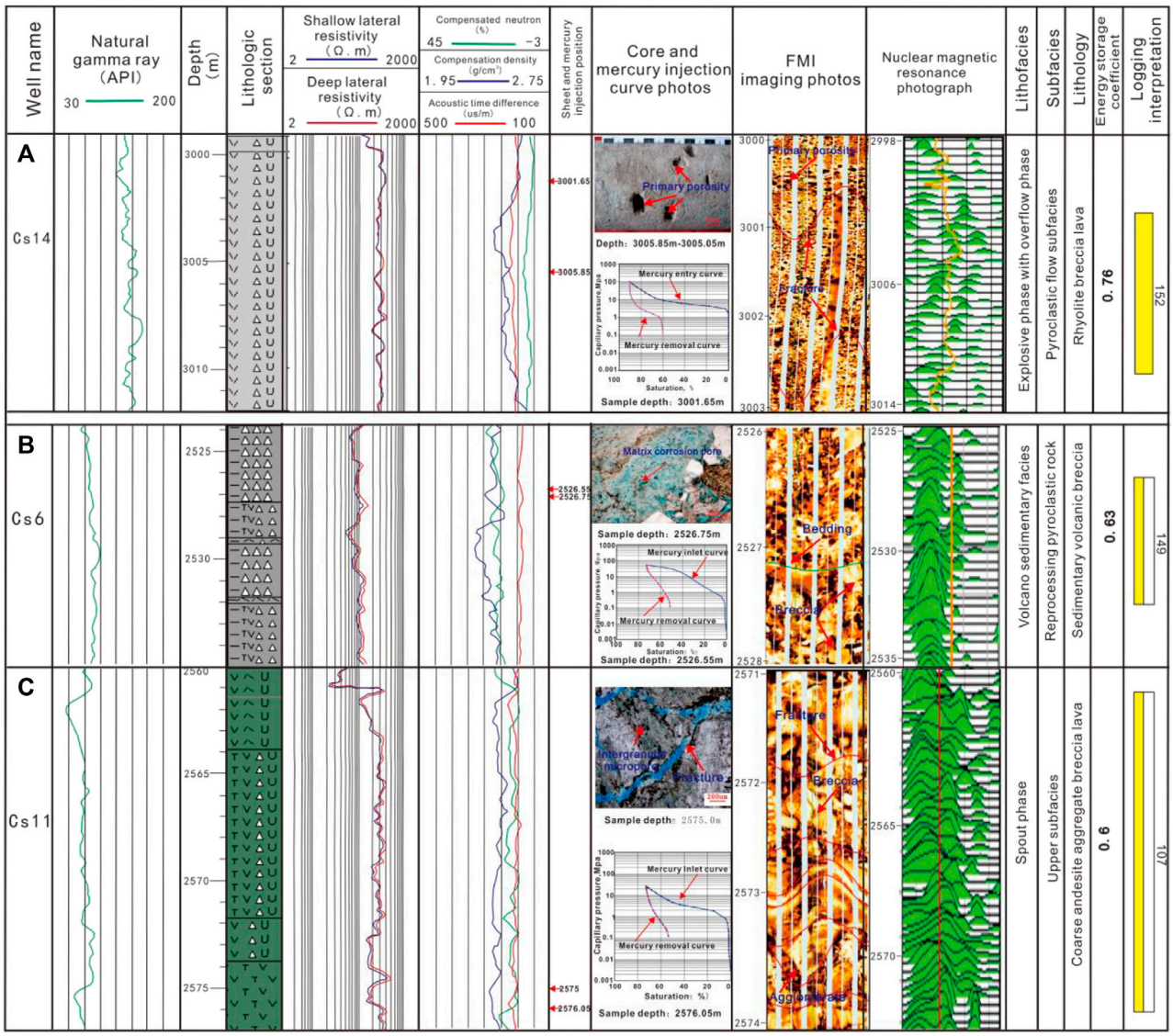

FIGURE 9 | Typical logging evaluation map of Type I volcano reservoir in the Wangfu Gas Field. Notes: **(A)** Well Cs14; **(B)** Well Cs6; **(C)** Well Cs11.

20 MPa), and high maximum mercury saturation (89.9–99.2%). The reservoir has good physical properties, porosity ranging between 8–12% and permeability more than 0.1 mD.

Type II: The curve shape range is a straight line with a slope angle between 45° and 60°. The platform section is not developed, medium skewness and general sorting. The characteristic parameters are higher displacement pressure (PD is 2 ~ 6 MPa), higher median pressure of mercury saturation (PD is 20–36 MPa), and lower maximum mercury saturation (75.2–85.5%). The physical properties of the reservoir are general, with porosity between 4 and 8% and permeability between 0.01 and 0.1 mD.

Type III: The curve shape is close to the right and up, the skewness is very fine, and the sorting is poor; the characteristic parameters are high displacement pressure (PD > 6 MPa), no median mercury saturation, and extremely low maximum mercury saturation (25–35%). The reservoir property is low, the porosity is less than 4%, and the permeability is less than 0.01 mD.

4.4 Logging Response Characteristics of Typical Reservoirs

The logging response characteristics of typical reservoirs are investigated in order to realize the reservoir classification evaluation of the whole well section, comprehensively analyze

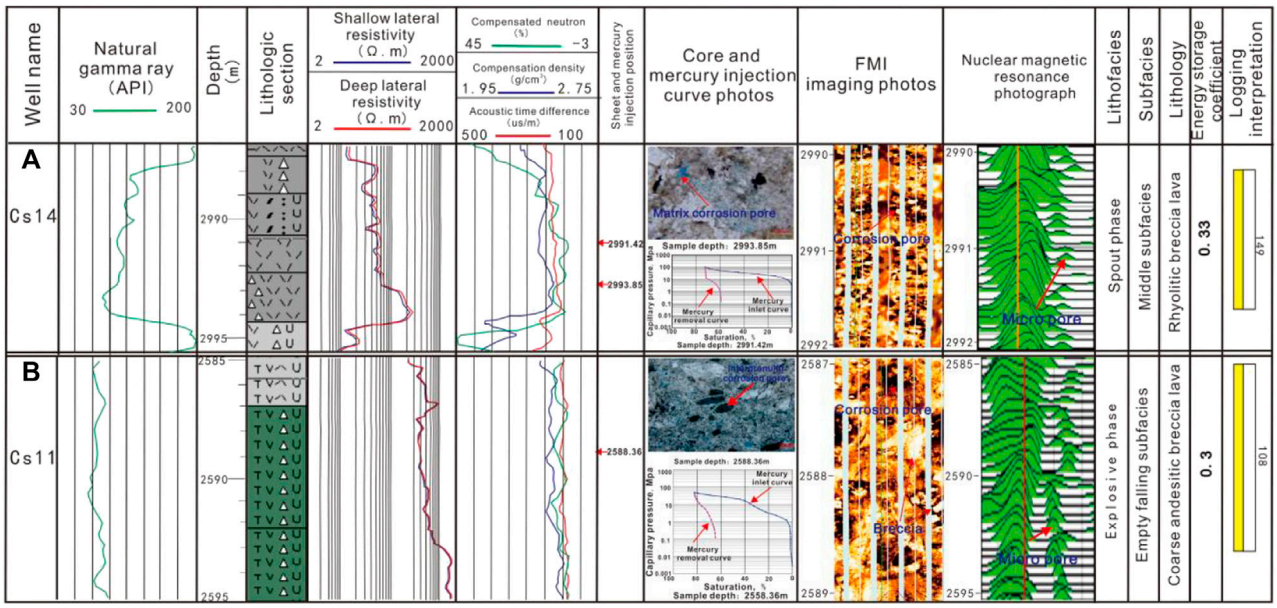

FIGURE 10 | Typical logging evaluation map for Type II volcano reservoir in the Wangfu Gas Field. Notes: **(A)** Well Cs14; **(B)** Well Cs11.

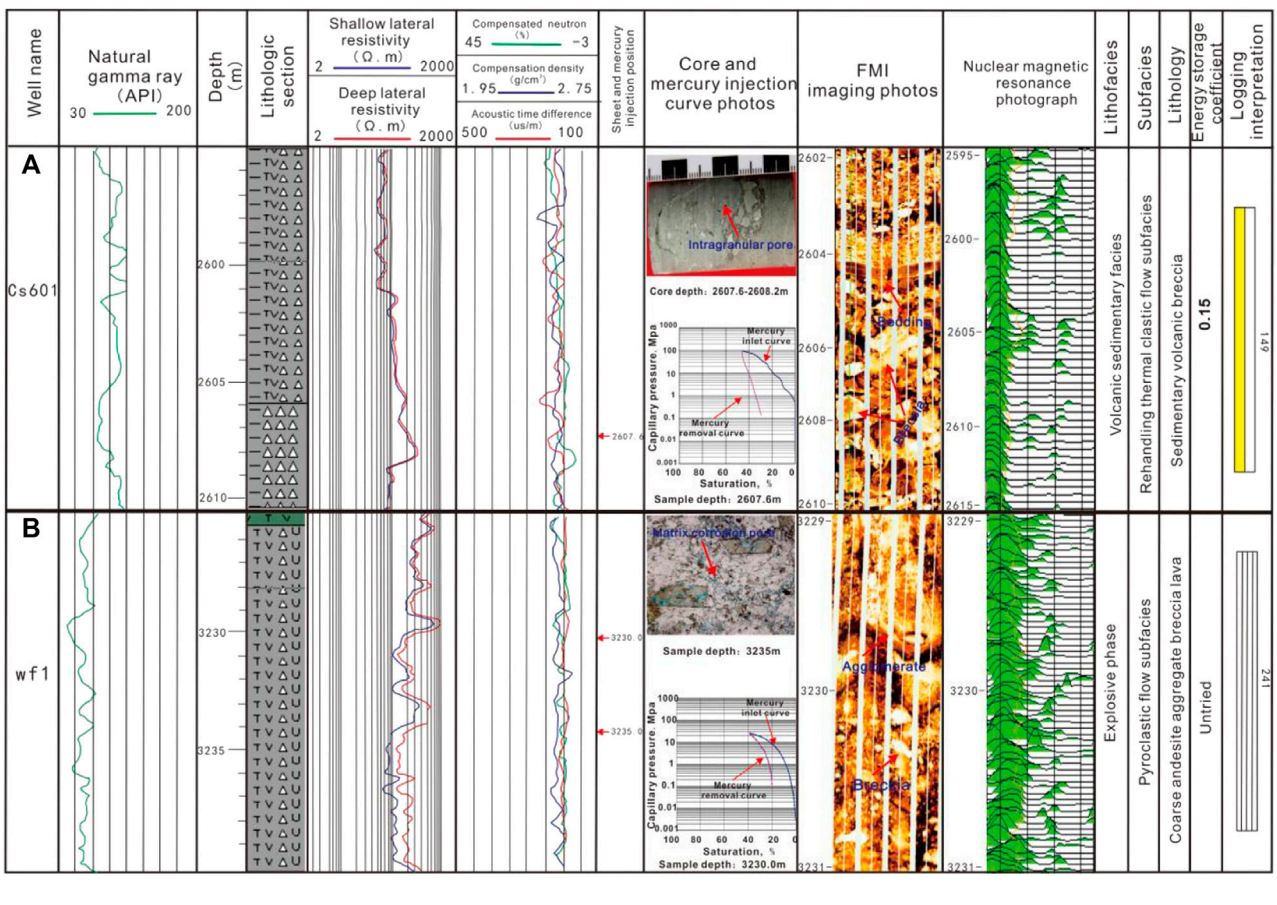

FIGURE 11 | Typical logging evaluation map of Type III volcano reservoir in the Wangfu Gas Field. Notes: **(A)** Well Cs601; **(B)** Well wf1.

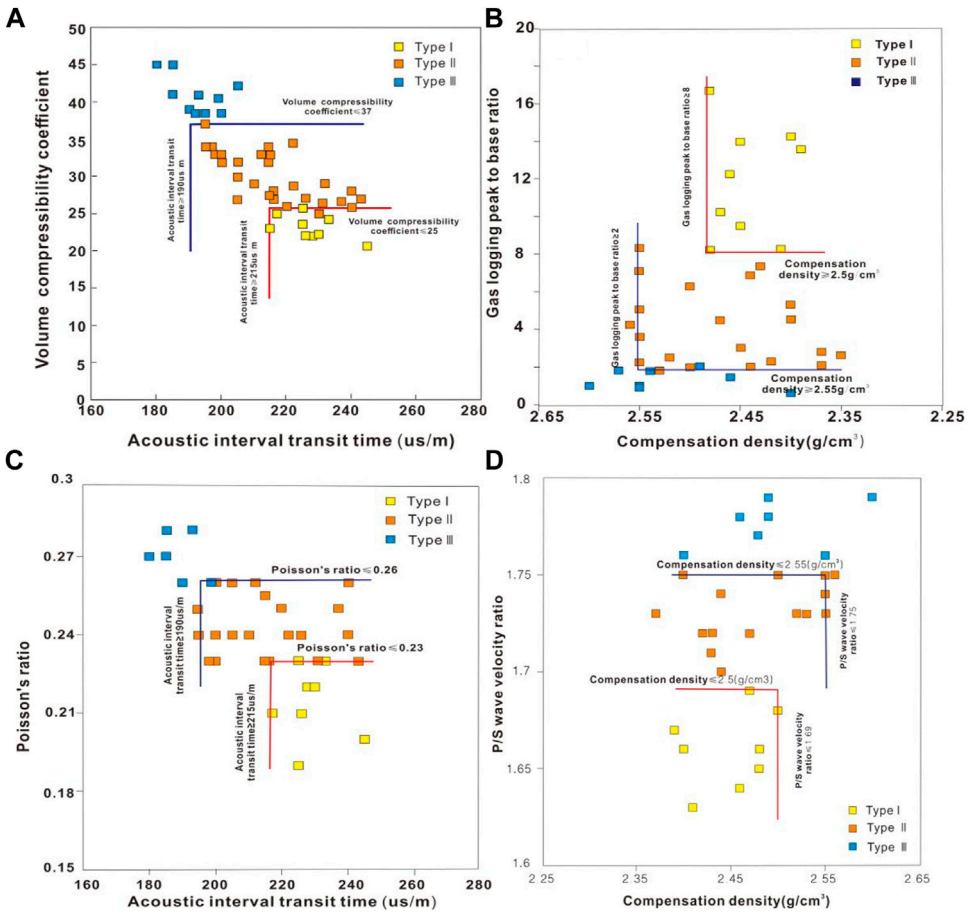

FIGURE 12 | Classification and identification chart of effective reservoir logging in the Wangfu gas field. Note: **(A)** Crossplot of the acoustic time difference and volume compressibility coefficient. **(B)** Compensated density-gas logging peak to base ratio crossplot. **(C)** Acoustic interval transit time Poisson's ratio crossplot. **(D)** Compensating density-P/S wave velocity ratio crossplot.

the conventional and special logging response characteristics, and summarize the logging response characteristics of different types of volcanic reservoirs.

Type I: Volcano lava reservoirs: Logging curves are characterized by high gamma ray (100–120 API), medium high resistivity (200–300 Ω m), high acoustic transit time, low density, and low neutron. FMI imaging shows the characteristics of stomata and high conductivity joints. NMR logging has common multi peak characteristics, and its free peaks develop. The T_2 spectrum is tailed obviously, as shown in **Figure 9A**. For the pyroclastic sedimentary rock reservoir, the logging curve shows low natural gamma (70–90API), medium resistivity (100–200 Ω m), low density, medium and low neutrons, an obvious excavation effect, a narrow strip shape, and a high acoustic time difference. FMI imaging shows the characteristics of agglomerates and breccia and certain bedding and fractures. Nuclear magnetic logging often shows double peak characteristics, and the amplitude of the free peak is large. The tailing phenomenon of the T_2 spectrum is obvious, as shown in **Figure 9B** and **Figure 9C**.

Type II: Volcano lava reservoirs: Logging curves are characterized by high gamma ray (90-115API), low resistivity (50–100 Ω m), low density, low neutron, a low acoustic time difference, and no obvious excavation effect. FMI imaging shows relatively less obvious dissolution characteristics, no cracks, and bedding characteristics. Nuclear magnetic logging is mostly unimodal, its free peaks are not developed, and the T_2 spectrum is not obvious, as shown in **Figure 10A**. For the volcanic lava reservoir, the logging curve shows high natural gamma (70–90API), medium and high resistivity (200–400 Ω m), low density, medium and low neutrons, and a low acoustic wave time difference, and the excavation effect is not obvious. Some breccia characteristics can be seen in FMI Imaging, but the breccia boundary is fuzzy, with certain fusion characteristics, no fracture, and bedding characteristics, and the nuclear magnetic logging mostly shows single peak characteristics, the free peak is not developed, and the tailing phenomenon of the T_2 spectrum is not obvious, as shown in **Figure 10B**.

Type III: The logging curve shows medium and low natural gamma (50–90 API). Due to the difference of breccia size and composition, the resistivity changes greatly (80–500 Ω m). The density ranges between high and medium, and almost no obvious excavation effect and low acoustic wave time

TABLE 4 | Classification standard of volcano reservoir in the Wangfu Gas Field.

Series & Category	Lithology and lithofacies		Reservoir physical properties		Microscopic characteristics			Conventional logging curve		Logging and logging data derived parameters				Special logging series		Productivity characteristics
	Lithology	lithofacies	Porosity (%)	Permeability (mD)	Displacement pressure (MPa)	Throat mean (m)	Median pressure (MPa)	AC (us/m)	Den (g/cm^3)	Gas logging peak to base ratio	Volume compressibility coefficient	P / S wave velocity ratio	Poisson's ratio	Nuclear magnetic logging	Imaging logging	
Type I	Volcanic lava, pyroclastic sedimentary rock	Explosive phase and overflow phase	>8	>0.1	<2	<12	<20	>215	<2.5	>8	<25	<1.69	<0.23	Common multimodal characteristics, free peak development, and T_2 spectrum tail phenomenon are obvious.	Pores, breccias and high guide fractures can be seen, and a small amount of bedding can be seen locally	The energy storage coefficient is greater than 0.6 and has a certain stable production capacity, with a daily gas output of more than 3.74 × 10^4m^3/d
Type II	Volcanic lava pyroclastic rock, pyroclastic rock sedimentary rock	Explosive facies, volcanic sedimentary facies	4–8	0.01–0.1	2–6	12–16	20–36	190–215	2.5–2.55	2–8	25–37	1.69–1.75	0.23–0.26	There is a single peak character, the free peak is not developed, and the T_2 spectrum is not obvious.	Relatively insignificant dissolution features can be seen, no fracture and bedding features are found, and some breccia boundaries are fuzzy	The energy storage coefficient is between 0.3–0.6, stable production capacity is poor, Nissan 1.62 – 3.74 × 10^4m^3/d
Type III	Volcanic lava, pyroclastic rock, volcanic lava pyroclastic rock, pyroclastic sedimentary rock	Explosive facies, overflow facies and volcanic sedimentary facies	<4	<0.01	>6	>16	>36	<190	>2.55	<1.8	>37	>1.75	>0.26	Nuclear magnetic logging is mostly characterized by single peak, and there is no tailing phenomenon of T_2 spectrum	Obvious characteristics of agglomerates and breccia can be seen, and the boundary of agglomerates or breccia is fuzzy	The energy storage coefficient is less than 0.3, the gas production is less, and the daily gas production is less than 1.62 × 10^4m^3/d

TABLE 5 | effective reservoir thickness, fracturing parameters, and process data table of Block CS6 in the Wangfu gas field.

Well Number	Effective Reservoir Thickness (m)				Fracturing Technology	Fracturing Parameters			Gas Volume (× $10^4 m^3/d$)
	Type I	Type II	Type III	Total Thickness		Number of Segments	Sand Quantity (m^3)	Liquid volume (m^3)	
CS6	11.6	19.2	18.2	49	Vertical well multi-stage fracture pattern fracturing	2	140	824.6	3.0
CS601	8.0	14.8	26.8	49.6	Vertical well multi-stage fracture pattern fracturing	2	110	763	0.58

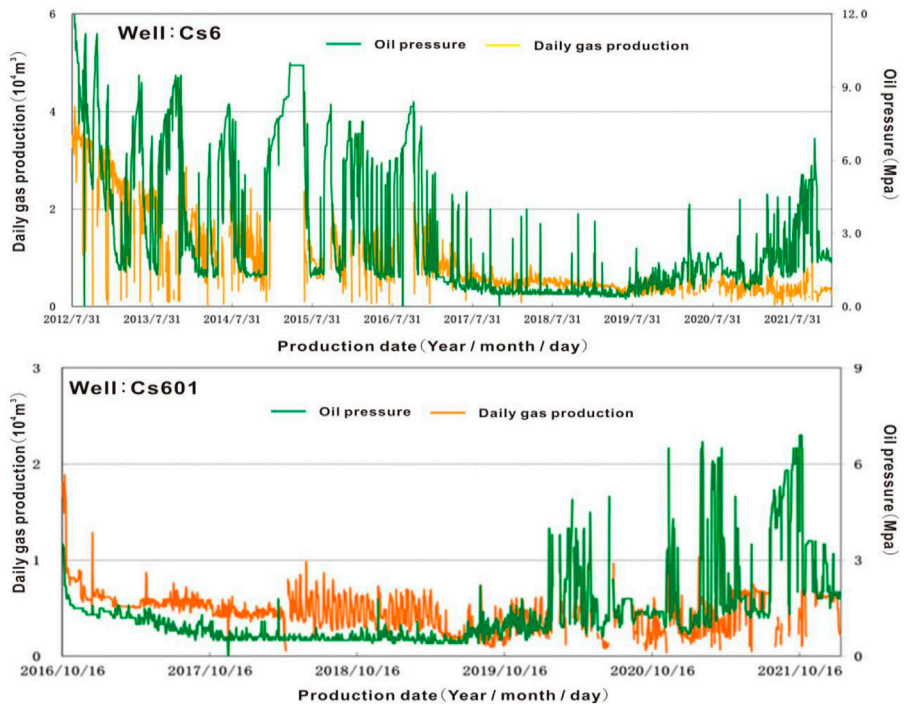

FIGURE 13 | production curve of wells CS6 and cs601 in the Wangfu gas field.

difference are observed; FMI imaging shows obvious lump and breccia characteristics. The blocks or breccia boundaries are fuzzy. They have certain melting characteristics, which reflect the tight characteristics of the reservoir. The nuclear magnetic logging is mostly single peak, as shown in **Figures 11A,B**.

4.5 Classification and Identification of Volcanic Reservoirs

The aim of this part is to summarize the logging response characteristics of the reservoir (**Figure 9**, **Figure 10** and **Figure 11**), analyze the corresponding relationship between logging and logging response characteristics of different types of reservoirs and physical properties and gas bearing properties, optimize the parameters such as the P/S wave velocity ratio (eliminate lithology lithologic effects, considering the difference of fluid on the influence of the longitudinal wave, shear wave velocity, and identification of reservoir hydrocarbon content), gas logging peak to base ratio (during logging, the ratio of the gas measurement peak value to base value is used to judge the reservoir gas content), volume compressibility coefficient (the difference in gas content leads to the change of the ratio of compressibility to compressibility, which is derived from the ratio of compressibility to compressibility), Poisson's ratio (the ratio of axial strain to radial strain indirectly reflects the gas bearing property of the reservoir, and this parameter is derived from the aspect ratio), acoustic interval transit time, and compensation density, establish the intersection chart of reservoir classification (**Figure 12**), and then determine the reservoir classification standard (**Table 4**).

The study equally comprehensively analyzes the laboratory and logging data, the reservoir classification chart (**Table 3** and **Table 4**) is established, and finally, a new set of volcanic reservoir classification standards is determined, as shown in **Table 4**.

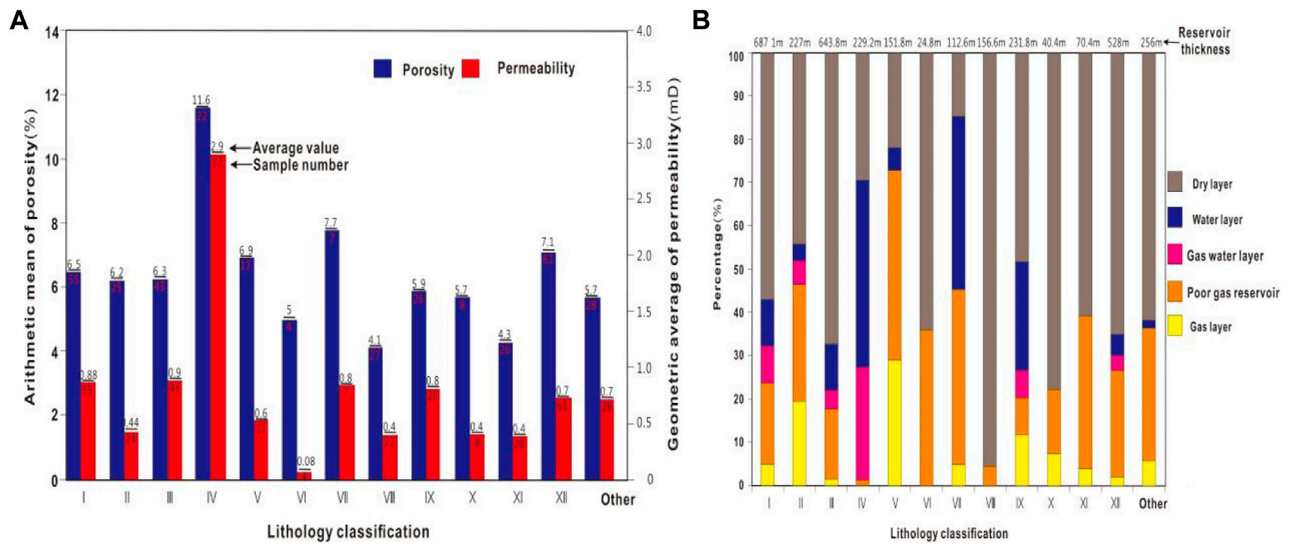

FIGURE 14 | Relationship between volcanic reservoir physical properties, effective reservoir distribution, and rock types. Notes: I—coarse andesite, II—coarse andesitic breccia lava, III—coarse andesitic volcanic breccia, IV—coarse andesitic tuff, V—rhyolite, VI—rhyolitic tuff lava, VII—trachyte, VIII—andesite, IX—andesitic volcanic breccia, X—andesitic tuff, XI—sedimentary tuff, and XII—sedimentary breccia. **(A)** Histogram of the lithology physical property relationship of the volcanic reservoir. **(B)** Histogram of the lithology effective reservoir relationship of the volcanic reservoir.

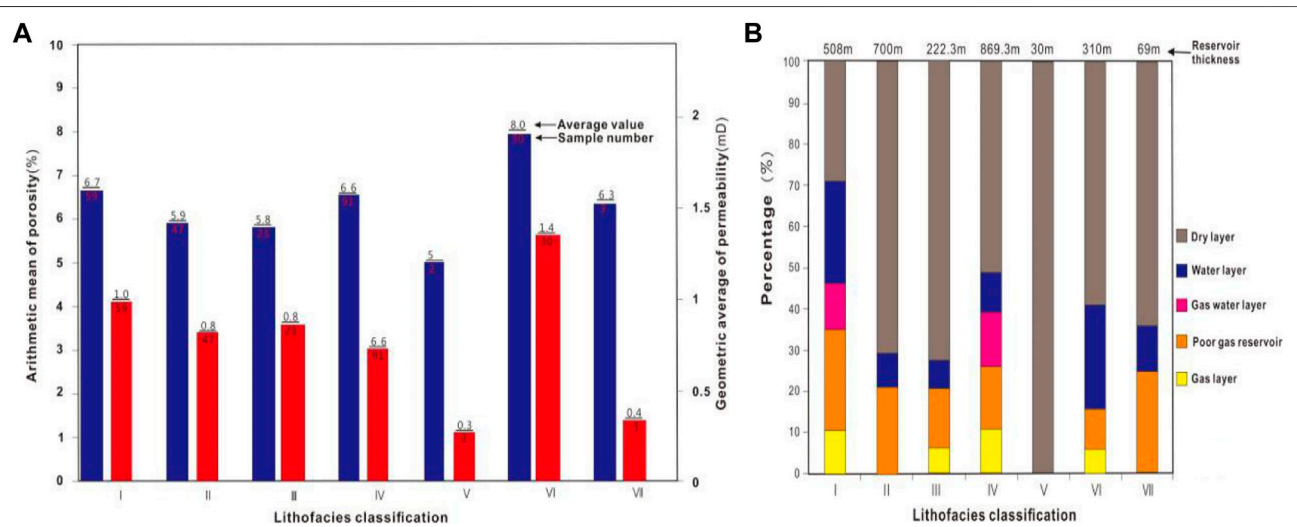

FIGURE 15 | Relationship between volcanic reservoir physical properties, effective reservoir distribution, and lithofacies type. Notes: I—upper subfacies, II—middle subfacies, III—lower subfacies, IV—thermal clastic flow subfacies, V—thermal wave subfacies, VI—air fall subfacies, and VII—volcanic neck subfacies. **(A)** Histogram of the lithofacies physical property relationship of the volcanic reservoir. **(B)** Histogram of the lithofacies effective reservoir relationship of the volcanic reservoir.

4.6 Result Verification

According to the above criteria, 29 wells are classified, and the accuracy of reservoir classification results is verified by gas test and production data. Wells CS6 and cs601 are two wells located in the same trap (**Figure 2**). The effective reservoir thickness produced is 49 and 49.6 m. It is approximately considered that the effective reservoir thickness produced is the same. The fracturing process and fracturing parameters adopted are basically the same, but the production effect is quite different (**Table 5** and **Figure 13**). The main reason for the analysis is that the thickness of type I and II reservoirs is relatively large in the CS6 well, which are 11.6 and 19.2 m, respectively, accounting for 62.8% of the total applied thickness. The type III reservoirs are relatively few, so the output of the CS6 well is relatively high. The reason for the low production of the CS601 well is mainly due to the use of type III reservoirs. The effective thickness of type I and II reservoirs is relatively thin, and the contribution of reservoir productivity is relatively small. Therefore, the results of the

operation confirm that the classification methods and results are relatively accurate.

5 DISCUSSION

5.1 Relationship Between Lithology, Lithofacies, and Effective Reservoir

5.1.1 Lithology, Physical Property, and Effective Reservoir

The volcano reservoir has strong heterogeneity, and different volcanic rocks have different properties such as density, composition, and structure, which lead to different physical properties of volcano rocks with different lithology. According to the measured physical property data, logging interpretation results, and gas test data, statistics are made on the reservoir physical properties and effective reservoir distribution of 12 main volcanic rocks developed in the Wangfu gas field. The results showed that the lithology with good physical properties is coarse andesite tuff, trachyte, and sedimentary breccia, followed by coarse andesite breccia lava, coarse andesite volcanic breccia, and rhyolite, and the lithology with poor physical properties is rhyolite tuff lava, andesite, andesite volcanic breccia, andesite tuff, and sedimentary tuff (**Figure 14A**). According to the comprehensive analysis of effective reservoir proportion and development thickness, effective reservoirs are mainly distributed in rhyolite, coarse andesite breccia lava, and trachyte, followed by coarse andesite, rhyolite tuff lava, tuff, and breccia, and effective reservoirs of other lithology are less developed (**Figure 14B**).

Forming two points: 1) The corresponding relationship between physical properties and gas bearing properties of reservoirs with the same lithology is poor. For example, coarse andesitic tuff has good physical properties, but its gas bearing properties are poor, and most of the effective reservoirs are class III reservoirs. Therefore, the development of effective reservoirs is greatly affected not only by reservoir physical properties but also by reservoir forming conditions and other factors. 2) The effective reservoirs of rhyolite, coarse andesite breccia lava, trachyte, and sedimentary breccia are relatively developed, especially the rhyolite reservoir. Class I and class II reservoirs account for more than 75% of the rhyolite reservoirs revealed in the whole region.

5.1.2 Lithofacies, Physical Properties, and Effective Reservoir

The physical characteristics of volcano facies are very different. According to the measured physical property data, logging interpretation results, and gas test data, the reservoir physical properties and effective reservoir distribution of the volcano facies reservoir developed in the Wangfu gas field are statistically analyzed. The results showed that the lithofacies with good physical properties are upper subfacies (I), thermal clastic flow subfacies (IV), and empty subfacies (VI), followed by middle subfacies (II) and lower subfacies (III) (**Figure 15A**). Thermal wave subfacies (V) and volcanic neck subfacies (VII) have poor reservoir physical properties. Effective reservoirs are mainly distributed in the upper subfacies, empty fall subfacies, and thermal clastic flow subfacies, followed by the middle subfacies, lower subfacies, volcanic neck subfacies, and thermal base wave subfacies (**Figure 15B**).

Forming two conclusions: 1) The physical properties and effective reservoir development degree of the same lithofacies reservoir correspond well, and the high-quality lithofacies type corresponds to good physical properties and gas bearing properties; 2) The upper subfacies, air drop subfacies, and thermal clastic flow subfacies are the dominant facies belt types of effective reservoirs.

5.2 Relationship Between Diagenesis Such as Weathering, Leaching, and Dissolution, and Effective Reservoir

5.2.1 Weathering and Leaching

Weathering and leaching have a great impact on the physical properties of the volcanic reservoir (Heap et al., 2014; Colombier et al., 2017). The analysis shows that the volcanic reservoir of the Wangfu gas field is mainly affected by weathering forest filtration in the following two aspects:

1) The weathering crust formed at the top of volcanic rock eruption cycle and eruption interval is a high-quality reservoir development area (**Figure 2**). For example, in the well section 2560–2576 m at the top of volcanic rock cycle of well CS11, coarse andesite aggregate breccia lava, andesite, andesite tuff lava, and other reservoirs in this well section are affected by weathering and leaching, with good physical properties and excellent reservoir forming conditions, and class I and II reservoirs are developed. Under the influence of atmosphere and surface water, the volcanic reservoir in the weathering crust development area is broken to form a series of micro-fractures. At the same time, chemical weathering such as dissolution, oxidation, hydration, and carbonation leads to the development of source dissolution pores (matrix dissolution pores and micro-fractures) in the volcanic reservoir, which greatly improves the reservoir performance of volcanic rocks (**Figure 9C**).
2) Under the influence of weathering and denudation, the volcanic reservoir in the high part of the structure accumulates rapidly to the trough area to form a high-quality sedimentary pyroclastic reservoir. According to the cast thin section and imaging data of the coring section of well CS6, the volcanic breccia in the sedimentary volcanic breccia reservoir is mostly supported by clastic particles, and the breccia is poorly sorted. It can be seen that the volcanic breccia has certain rounding characteristics locally, and the matrix dissolution pores, phenocryst dissolution pores, and other secondary pores are developed (**Figure 2**, **Figure 9B**, **Figures 5E,F**). The physical properties of the reservoir are good. Class I, II, and III reservoirs are developed, with the porosity of 5–10% and the permeability of 0.01–1.17 mD. Weathering and denudation are the key to the formation of effective reservoirs of sedimentary pyroclastic rocks in high parts and control the distribution of sedimentary pyroclastic reservoirs in low parts.

5.2.2 Dissolution

The volcano reservoir has deep buried and long reservoir forming time, and most of them have experienced severe dissolution. Dissolution plays a significant role in improving

volcano reservoir formation (Li et al., 2014; Zhang et al., 2015). Core description and microscopic thin section identification show that the dissolution is mainly manifested in the dissolution of volcanic phenocrysts and matrix, and the dissolution of fillings in primary pores and fractures (**Figure 5E–G**). Dissolution pores are an important part of volcanic reservoir space in the study area. Class I, class II, and class III reservoirs are developed.

The dissolution of the volcano reservoir in this area has two advantages: 1) volcano rock forming stage experienced multi-stage tectonic movement, and faults and microfractures developed, providing channels for the migration of underground hydrothermal and acidic fluids. 2) Two sets of high-quality source rocks are developed at the interval of the volcanic eruption cycle and the bottom of the Shahezi Formation. In the thermal evolution stage, a large number of organic acid solutions can be formed, which is the key to dissolution. Therefore, there are secondary dissolution pore development zones formed by dissolution near the fault, the lower part of the unconformity and the top of the cycle.

6 CONCLUSION

1) The parameters such as effective thickness, effective thickness * porosity, formation coefficient, and energy storage coefficient are relatively sensitive to the productivity of gas wells, and the energy storage coefficient can better characterize the productivity of single wells of gas wells than other parameters, According to the boundary of energy storage coefficient greater than 0.6, 0.6–0.3, and less than 0.3, the volcano reservoir in the Wangfu gas field is subdivided into three types.
2) Taking the classification of the reservoir coefficient as the constraint condition, a series of experimental analysis work such as core observation, cast thin section, and conventional mercury injection are carried out for different types of reservoirs and the characteristics of different types of reservoirs are defined. In terms of reservoir space combination characteristics, the Type I reservoir is mainly composed of structural fracture matrix dissolution pores, structural fracture matrix micropores, and matrix dissolution pores. Type II reservoir matrix dissolution pores and residual intergranular pores are relatively developed, and the Type III reservoir is mainly composed of structural fractures. In terms of micro-pore structure characteristics, from Type I to Type III reservoirs, the porosity, permeability, and maximum mercury saturation decreased, the displacement pressure and median saturation pressure increased. From class I to class III reservoirs, the shape skewness and sorting coefficient of mercury injection curve deteriorated.
3) There are some differences in the logging curve characteristics of different typical reservoirs. Among them, the derived parameters such as P-and S-wave velocity, peak to base ratio of gas logging, volume compressibility coefficient, acoustic time difference, and density are relatively sensitive to reservoir characteristics. Based on the above parameters, four sets of reservoir classification charts were established, and 29 reservoirs in the whole area were classified and evaluated. The results of gas well test in Cs6, Cs601, and other wells confirmed that the classification standards were accurate and reliable.
4) Weathering, leaching, dissolution, and other diagenesis have improved the physical properties of the reservoir. The corresponding relationship between lithology, physical property, and gas bearing property is poor, which shows that the development degree of the effective reservoir is not only controlled by lithology but also affected by reservoir space type, diagenesis, and other factors. Lithologic facies correspond well with physical properties and gas bearing properties of reservoirs. Rhyolitic, coarse, and stable breccia lava, trachyte, and sedimentary breccia are relatively effective lithologic reservoirs. The lithofacies of Kobe Aso, air fall subfacies, and thermal clastic flow are the dominant facies belts of effective reservoirs.

DATA AVAILABILITY STATEMENT

The original contributions presented in the study are included in the article/Supplementary Material; further inquiries can be directed to the corresponding author.

AUTHOR CONTRIBUTIONS

W-TS: The leading author of this article. Z-HL: Funding provider. Y-SL: Guide teachers and provide overall thinking. LZ: funding provider, experimental operator and drawing personnel. H-MW: Data analyst and article checker. AK: data analyst and article checker.

FUNDING

This work was completed with the support of China's major national special project "development of large oil and gas fields and coalbed methane" special topic "effective development technology of deep tight gas in the south of Songliao Basin" (2016zx05047005-006).

ACKNOWLEDGMENTS

We thank Professor Lou Yishan and Professor Li Zhonghui for their technical guidance. At the same time, the author thanks Professor Tang Huafeng's team of Jilin University for their analytical and laboratory equipment and their professionals for their useful advice, discussion, and help. We also thank the reviewers for their comments.

REFERENCES

Chang, X., Wang, Y., Shi, B., and Xu, Y. (2019). Charging of Carboniferous Volcanic Reservoirs in the Eastern Chepaizi Uplift, Junggar Basin (Northwestern China) Constrained by Oil Geochemistry and Fluid Inclusion. *Bulletin* 103 (7), 1625–1652. doi:10.1306/12171818041

Chen, H. Q., Hu, Y. L., Yan, L., Zhang, J., and Tong, M., (2016). Comprehensive Quantitative Evaluation of Yingchengl Volcanic Reservoirs in Xudong. *Special oil gas Reserv.* 23 (01), 21–24. doi:10.3969/j.issn.1006-6535.2016.01.005

Chen, K. Y., Duan, X. G., Zhang, X. B., and Song, R. C. (2010). Lithology Identification and Prediction of Igneous Rock Based on 3D Lithofacies Simulation. *Joumal Southwest Petrolerm Univ. Sci. Technopgy Ed.* 32 (02), 19–24. doi:10.3863/j.issn.1674-5086.2010.02.004

Colombier, M., Wadsworth, F. B., Gurioli, L., Scheu, B., Kueppers, U., Di Muro, A., et al. (2017). The Evolution of Pore Connectivity in Volcanic Rocks. *Earth Planet. Sci. Lett.* 462, 99–109. doi:10.1016/j.epsl.2017.01.011

Faizan, N., Löffler, A., Heininger, R., Utesch, M., and Krcmar, H. (2019). Classification of Evaluation Methods for the Effective Assessment of Simulation Games: Results from a Literature Review. *Int. Assoc. Online Eng.* Retrieved from. www.learntechlib.org/p/207576/ March 4, 2022. 9(1), doi:10.3991/ijep.v9i1.9948

Farquharson, J., Heap, M. J., Varley, N. R., Baud, P., and Reuschlé, T. (2015). Permeability and Porosity Relationships of Edifice-Forming Andesites: a Combined Field and Laboratory Study. *J. Volcanol. Geotherm. Res.* 297, 52–68. doi:10.1016/j.jvolgeores.2015.03.016

Feng, Z. Q. (2006). Exploration Prospect of Qingshen Large Gas Field in Songliao Basin. *Nat. Gas. Ind.* 25 (06), 1–5.

Feng, Z. Q. (2008). Volcanic Rocks as Prolific Gas Reservoir: A Case Study from the Qingshen Gas Field in the Songliao Basin, NE China. *Mar. Petroleum Geol.* 25 (4-5), 416–432. doi:10.1016/j.marpetgeo.2008.01.008

Feng, Z., Yin, C., Liu, J., Zhu, Y., Lu, J., and Li, J. (2014). Formation Mechanism of In-Situ Volcanic Reservoirs in Eastern China: A Case Study from Xushen Gasfield in Songliao Basin. *Sci. China Earth Sci.* 57, 2998–3014. doi:10.1007/s11430-014-4969-2

Gao, F. (2019). Use of Numerical Modeling for Analyzing Rock Mechanic Problems in Underground Coal Mine Practices. *J. Min. Strata Control Eng.* 1 (1), 013004. doi:10.13532/j.jmsce.cn10-1638/td.2019.02.009

Gong, Q. S., Huang, G. P., Meng, X. C., Zhu, C., and Ni, G. H. (2012). Methods for Lithology Discrimination of Volcanics in Santanghu Basin. *China pet. Explor.* 17 (03), 37–41+6. doi:10.3969/j.issn.1672-7703.2012.03.006

Hasan, A., Baroudi, B., Elmualim, A., and Rameezdeen, R. (2018). Factors Affecting Construction Productivity: a 30 Year Systematic Review. *Ecam* 25 (7), 916–937. doi:10.1108/ecam-02-2017-0035

He, H., Li, S. M., Kong, C. X., Jiang, Q. P., Zhou, T. Y., Jia, J. F., et al. (2016). Characteristics and Quantitative Evaluation of Volcanic Effective Reservoir in Jiamuhe Formation of Permian, Northwestern Margin of Junggar Basin. *J. China Univ. Petroleum Nat. Sci.* 40 (02), 1–12. doi:10.3969/j.issn.1673-5005.2016.02.001

Heap, M. J., Xu, T., and Chen, C. F. (2014). The Influence of Porosity and Vesicle Size on the Brittle Strength of Volcanic Rocks and Magma. *Bull. Volcanol.* 76 (9), 1–15. doi:10.1007/s00445-014-0856-0

Hou, E., Cong, T., Xie, X., and Wei, J. B. (2020). Ground Surface Fracture Development Characteristics of Shallow Double Coal Seam Staggered Mining Based on Particle Flow. *J. Min. Strata Control Eng.* 2 (1), 013521. doi:10.13532/j.jmsce.cn10-1638/td.2020.01.002

Huang, Y. X., Hu, W. S., Yuan, B. T., Zhang, G. Y., and Bai, L. D. (2019). Evaluation of Pore Structures in Volcanic Reservoirs: a Case Study of the Lower Cretaceous Yingcheng Formation in the Southern Songliao Basin, NE China. *Environ. Earth Sci.* 78 (4), 1–14. doi:10.1007/s12665-019-8055-0

Jin, C. Z., Yang, S. L., Shu, P., and Wang, G. J. (2007). Comprehensive Research on Relationship between Productivity and Pore Structure Characteristics of Volcanic Reservoir in Shengping Developing Area. *Petroleum Geol. Oilfield Dev. Daqing* 26 (2), 38–45. doi:10.3969/j.issn.1000-3754.2007.02.010

Kadavi, P. R., and Lee, C.-W. (2018). Land Cover Classification Analysis of Volcanic Island in Aleutian Arc Using an Artificial Neural Network (ANN) and a Support Vector Machine (SVM) from Landsat Imagery. *Geosci. J.* 22 (4), 653–665. doi:10.1007/s12303-018-0023-2

Lan, S. R., Song, D. Z., Li, Z. L., and Liu, Y. (2021). Experimental Study on Acoustic Emission Characteristics of Fault Slip Process Based on Damage Factor. *J. Min. Strata Control Eng.* 3 (3), 033024. doi:10.13532/j.jmsce.cn10-1638/td.20210510.002

Li, G. R., Wu, H. Z., Ye, B., Li, Z. Z., Peng, B., and Wu, Y. J. (2014). Stages and Mechanism of Dissolution in Changhsing Reservoir, Yuanba Area. *Acta Petrol. Sin.* 30 (03), 709–717. doi:10.3787/j.issn.1000-0976.2017.02.007

Li, H. (2022). Research Progress on Evaluation Methods and Factors Influencing Shale Brittleness: A Review. *Rep.* 8, 4344–4358. doi:10.1016/j.egyr.2022.03.120

Li, X., Song, M., Lin, H., Zhang, K., Shi, H., Zhang, Y., et al. (2019). Characteristics of Carboniferous Volcanic Reservoirs in the Chun-Feng Oilfield of the Junggar Basin, China. *Arabian J. Geosciences* 12 (16), 1–13. doi:10.1007/s12517-019-4663-y

Liu, W. F., and Kuang, H. W. (2003). Comprehensive Evaluation of Volcanics Reservoir by Fuzzy Mathematics. *Oil Gas Recovery Technol* 10 (2), 1–5. doi:10.13673/j.cnki.cn37-1359/te.2003.02.003

Luo, J. L., Lin, T., Yang, Z. S., Liu, X. H., Zhang, J., and Liu, S. Y. (2008). Lithofacies and Reservoir Quality Control Factors of Volcanics in the YingchengFormation in the Shengping Gas Field in the Songliao Basin. *Oil & Gas Geol.* 29 (06), 748–757. doi:10.3321/j.issn:0253-9985.2008.06.007

Ma, S. W., Luo, J. l., Chen, C. Y., He, X. Y., Dai, J. J., Xu, X. L., et al. (2017). Classification and Evaluation of Micro Pore Structure of Volcanic Rock Reservoirs :A Case Study of the Carboniferous Volcanic Reservoirs in Xiquan Area, Eastern Junggar Basin. *Pet. geology & Exp.* 39 (05), 647–654. doi:10.11781/sysydz201705647

Mao, Z.-G., Zhu, R.-K., Luo, J.-L., Wang, J.-H., Du, Z.-H., Su, L., et al. (2015). Reservoir Characteristics, Formation Mechanisms and Petroleum Exploration Potential of Volcanic Rocks in China. *Pet. Sci.* 12 (1), 54–66. doi:10.1007/s12182-014-0013-6

Mou, Z. H., Liu, J. S., and Xu, J. (2010). Lithofacies of Volcanic Rock at the Top of Upper Carboniferous Stratigraphy in Luxi Area of Junggar Basin. *Nat. Gas. Geosci.* 21 (01), 47–53.

Pang, Y. M., Zhang, F. Q., Qiu, H. F., and Zhan, J. F. (2007). Characteristics of Microscopic Pore Structure and Physical Property Parameter in Acidic Volcanic Reservoir. *Acta Pet. Sin.* 28 (6), 72–77. doi:10.3321/j.issn:0253-2697.2007.06.014

Pola, A., Crosta, G., Fusi, N., Barberini, V., and Norini, G. (2012). Influence of Alteration on Physical Properties of Volcanic Rocks. *Tectonophysics,* 566-567, 67–86. doi:10.1016/j.tecto.2012.07.017

Polyansky, O. P., Reverdatto, V. V., Khomenko, A. V., and Kuznetsova, E. N. (2003). Modeling of Fluid Flow and Heat Transfer Induced by Basaltic Near-Surface Magmatism in the Lena-Tunguska Petroleum Basin (Eastern Siberia, Russia). *J. Geochem. Explor.* 78, 687–692. doi:10.1016/s0375-6742(03)00079-7

Ran, Q. Q., Hu, Y. L., and Ren, B. S. (2005). A Lithologic Identification Method of Igneous Rocks and its Application: a Case of the Igneousreservoir in Block Zao-35. *China offshore oil gas* 23 (3), 25–30. doi:10.3969/j.issn.1673-1506.2005.01.006

Ren, Z. W., and Jin, C. S. (1999). Reservoir Space Feature of the Volcanic Rocks in the Area of WellWa-609, Liaohe Sag. *Petroleum Explor. Dev.* 26 (04), 54–56 + 5. doi:10.1006/mcpr.1998.0211

Shan, X. L., Chen, Y. P., Tang, L. M., and Yi, J. (2011). Comprehensive Evaluation Method for Volcanic Rock Reservoirs and Its Application: Taking Songnan Gas Field for Example. *J. Shandong Univ. Sci. Technol. Nat. Sci.* 30 (03), 1–6. doi:10.3969/j.issn.1672-3767.2011.03.001

Shi, B., Chang, X., Xu, Y., Mao, L., Zhang, J., and Li, Y. (2020). Charging History and Fluid Evolution for the Carboniferous Volcanic Reservoirs in the Western Chepaizi Uplift of Junggar Basin as Determined by Fluid Inclusions and Basin Modelling. *Geol. J.* 55 (4), 2591–2614. doi:10.1002/gj.3527

Shi, X. L., Cui, Y. J., Xun, W. K., Zhang, J. S., and Guan, Y. Q. (2020). Formation Permeability Evaluation and Productivity Prediction Based on Mobility from Pressure Measurement while Drilling. *Petroleum Explor. Dev.*, 47(1), 146–153. doi:10.1016/S1876-3804(20)60013-1

Sruoga, P., Rubinstein, N., and Hinterwimmer, G. (2004). Porosity and Permeability in Volcanic Rocks: a Case Study on the Serie Tobífera, South Patagonia, Argentina. *J. Volcanol. Geotherm. Res.*, 132(1), 31–43. doi:10.1016/S0377-0273(03)00419-0

Sruoga, P., and Rubinstein, N. (2007). Processes Controlling Porosity and Permeability in Volcanic Reservoirs from the Austral and Neuquén Basins, Argentina. *Bulletin* 91 (1), 115–129. doi:10.1306/08290605173

Stagpoole, V., and Funnell, R. (2001). Arc Magmatism and Hydrocarbon Generation in the Northern Taranaki Basin, New Zealand. *Pet. Geosci.* 7(3), 255–267. doi:10.1144/petgeo.7.3.255

Sun, H., Zhong, D., and Zhan, W. (2019). Reservoir Characteristics in the Cretaceous Volcanic Rocks of Songliao Basin, China: A Case of Dynamics and Evolution of the Volcano-Porosity and Diagenesis. *Energy Explor. Exploitation*, 37(2), 607–625. doi:10.1177/0144598718812546

Tang, H. F., Wang, P. J., and Bian, W. H. (2020). Review of Volcanic Reservoir Geology. *Acta Pet. Sin.* 41 (12), 1744–1773. doi:10.7623/syxb202012026

Tian, J., Sun, X., Zhang, X., and Shou, Y. (2013). Reservoir Space Types and the Factors Influencing the Characteristics of Spherulite in Rhyolite. *Sci. China Earth Sci.* 56(5), 748–755. doi:10.1007/s11430-013-4599-0

Wang, L., He, Y., Peng, X., Deng, H., Liu, Y., and Xu, W. (2020). Pore Structure Characteristics of an Ultradeep Carbonate Gas Reservoir and Their Effects on Gas Storage and Percolation Capacities in the Deng IV Member, Gaoshiti-Moxi Area, Sichuan Basin, SW China. *Mar. Petroleum Geol.* 111, 44–65. doi:10.1016/j.marpetgeo.2019.08.012

Wang, L., Li, J. H., Shi, Y. M., Zhao, Y., and Ma, Y. S. (2014). Analysis of the Reservoir Spaces and Their Main Controlling Factors of Carboniferous Volcanic Rocks in Dixi Area, Junggar Basin. *Earth. Sci. Front.* 21 (1), 205.

Wang, P., and Chen, S. (2015). Cretaceous Volcanic Reservoirs and Their Exploration in the Songliao Basin, Northeast China. *Bulletin*, 99(3), 499–523. doi:10.1306/09041413095

Wang, P. J., Chen, S. M., Liu, W. Z., Shan, X. L., Cheng, R. H., Zhang, Y., et al. (2003b). Relationship between Volcanic Facies and Volcanic Reservoirs in Songliao Basin. *Oil Gas Geol.* 24 (1), 18–23. doi:10.3969/j.issn.1671-5888.2003.04.011

Wang, P. J., Chi, Y. L., Liu, W. Z., Cheng, R. H., Shan, X. L., and Ren, Y. G. (2003a). Volcanic Facies of the Songliao Basin: Classification, Characteristics and Reservoir Significance. *J. Jilin Univ. (Earth Sci. Ed.)* 33 (4), 449–456. doi:10.3969/j.issn.1671-5888.2003.04.011

Wang, P. J., Wu, H. Y., Pang, Y. M., Men, G. T., Ren, Y. G., Liu, W. Z., et al. (2006). Volcanic Facies of the Songliao Basin: Sequence, Model and the Quantitative Relationship with Porosity & Permeability of the Volcanic Reservoir. *J. Jilin Univ. (Earth Sci. Ed.)* 36 (5), 805–812. doi:10.3969/j.issn.1671-5888.2006.05.016

Wang, Y., Gao, Y., and Fang, Z. (2021). Pore Throat Structure and Classification of Paleogene Tight Reservoirs in Jiyang Depression, Bohai Bay Basin, China. *Petroleum Explor. Dev.*, 48(2), 308–322. doi:10.1016/S1876-3804(21)60025-3

Wang, Z. S., Liu, Z. C., Du, Y. L., Tan, Z. H., Hu, J. G., Yang, S. H., et al. (2016). A Splitting Method of Oil and Gas Production in Multiple Completion Wells of Multi Layered Reservoir. *Nat. Gas. Geosci.* 27 (10), 1878–1882. doi:10.11764/j.issn.1672-1926.2016.10.1878

Wen, L., Li, Y., Yi, H., Liu, X., Zhang, B., Qiu, Y., et al. (2019). Lithofacies and Reservoir Characteristics of Permian Volcanic Rocks in the Sichuan Basin. *Nat. Gas. Ind. B*, 6(5), 452–462. doi:10.1016/j.ngib.2019.02.003

Wu, C., Gu, L., Zhang, Z., Ren, Z., Chen, Z., and Li, W. (2006). Formation Mechanisms of Hydrocarbon Reservoirs Associated with Volcanic and Subvolcanic Intrusive Rocks: Examples in Mesozoic-Cenozoic Basins of Eastern China. *Bulletin* 90 (1), 137–147. doi:10.1306/07130505004

Yang, Z. P., Yue, S. J., Zheng, C. L., Liu, X. Z., and Chen, G. X. (2018). Production Split Method Restricted Synthetically by Multi-Factors in Thin Interbed Sandstone Reservoirs. *Lithol. Reserv.* 30 (06), 117–124. doi:10.12108/yxyqc.20180614

Yin, S., and Wu, Z. (2020). Geomechanical Simulation of Low-Order Fracture of Tight Sandstone. *Mar. Petroleum Geol.* 117, 104359. doi:10.1016/j.marpetgeo.2020.104359

Yu, C. M., Zheng, J. P., Tang, Y., Yang, Z., and Qi, X. F. (2004). Reservoir Properties and Effect Factors on Volcanic Rocks of Basement beneath Wucaiwan Depression, Junggar Basin. *Earth Sci.* 29 (5), 303–308. doi:10.3321/j.issn:1000-2383.2004.03.007

Zhang, K. H., Lin, H. X., Zhang, G. L., and Xu, W. L. (2015). Characteristics and Controlling Factors of Volcanic Reservoirs of Hala' Alate Mountains Tectonic Belt. *J. China Univ. Petroleum Nat. Sci.* 39 (02), 16–22. doi:10.3969/j.issn.1673-5005.2015.02.003

Zhao, J. Z., Wu, S. B., and Wu, F. L. (2007). The Classification and Evaluation Criterion of Low Permeability Reservoir: An Example from Ordos Basin. *Lithol. Reserv.* 19 (03), 28–31. doi:10.3969/j.issn.1673-8926.2007.03.005

Zheng, H., Sun, X., Wang, J., Zhu, D., and Zhang, X. (2018a). Devitrification Pores and Their Contribution to Volcanic Reservoirs: A Case Study in the Hailar Basin, NE China. *Mar. Petroleum Geol.*, 98, 718–732. doi:10.1016/j.marpetgeo.2018.09.016

Zheng, H., Sun, X., Zhu, D., Tian, J., Wang, P., and Zhang, X. (2018b). Characteristics and Factors Controlling Reservoir Space in the Cretaceous Volcanic Rocks of the Hailar Basin, NE China. *Mar. Petroleum Geol.*, 91, 749–763. doi:10.1016/j.marpetgeo.2018.01.038

Zhou, X. M., and Tang, Y. H. (2007). Productivity Characteristics and Influential Factors Analysis of Volcanic Gas Reservoirof Xushen Gas Field. *Nat. Gas. Ind.* 27 (01), 90–92. doi:10.3321/j.issn:1000-0976.2007.01.027

Conflict of Interest: W-TS was employed by the Company Exploration and Development Research Institute of Jilin Oil Field Company.

The remaining authors declare that the research was conducted in the absence of any commercial or financial relationships that could be construed as a potential conflict of interest.